ACS Chemical Neuroscience

Research Article

pubs.acs.org/chemneuro

Optimization of 6-Heterocyclic-2-(1*H*-pyrazol-1-yl)-*N*-(pyridin-2-yl)pyrimidin-4-amine as Potent Adenosine A_{2A} Receptor Antagonists for the Treatment of Parkinson's Disease

Jiyue Zheng,[†] Zhaohui Yang,[†] Xuan Li, Linlang Li, Haikuo Ma, Meiyu Wang, Hongjian Zhang, Xuechu Zhen,* and Xiaohu Zhang*

Jiangsu Key Laboratory of Translational Research and Therapy for Neuro-Psycho-Diseases and College of Pharmaceutical Sciences, Soochow University, Su Zhou, Jiangsu 215021, P. R. China

Supporting Information

ABSTRACT: Parkinson's disease is a neurodegenerative disease characterized by the motor symptoms of bradykinesia, tremor, and rigidity. Current therapies are based mainly on dopaminergic replacement strategies by administration of either dopamine agonists or dopamine precursor levodopa (L-Dopa). These treatments provide symptomatic relief without slowing or stopping the disease progression, and long-term usage of these drugs is associated with diminished efficacy, motor fluctuation, and dyskinisia. Unfortunately, there had been few novel treatments developed in the past decades. Among nondopaminergic strategies for the treatment of Parkinson's disease, antagonism of the adenosine A_{2A} receptor has emerged to show great potential. Here we report the optimization of a new chemical scaffold, which achieved exceptional receptor binding affinity and ligand efficiency against adenosine A_{2A} receptor. The leading compounds demonstrated excellent efficacy in the haloperidol induced catalepsy model for Parkinson's disease.

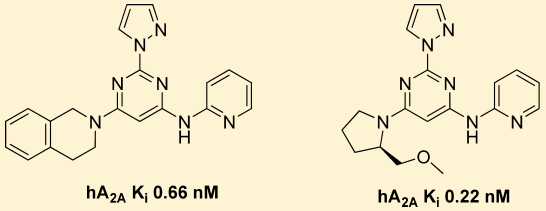

KEYWORDS: *Adenosine receptor, antagonist, GPCR, Parkinson's disease, lead optimization*

Parkinson's disease is a neurodegenerative disease that affects about 1.5% of the population over the age of 60.[1] As the world population ages and life expectancy increases, the number of individuals afflicted by Parkinson's disease is expected to double by 2030.[2] Unfortunately, there had been few novel treatments developed in the past decades. Current therapies are based mainly on dopaminergic replacement strategies by administration of either dopamine agonists or dopamine precursor levodopa (L-Dopa). These treatments provide symptomatic relief without slowing or stopping the disease progression, and long-term usage of these drugs is associated with diminished efficacy, motor fluctuation, and dyskinisia.[3,4] Furthermore, the current available dopaminergic drugs have very limited effects for the treatment of nonmotor symptoms of Parkinson's disease such as depression, dementia, sleep disorder, and other autonomic dysfunctions.[5] There is an urgent need to develop effective and durable symptomatic and disease-modifying therapies for the long-term management of Parkinson's disease.

Among nondopaminergic strategies for the treatment of Parkinson's disease, antagonism of the adenosine A_{2A} receptor has emerged to show great potential. Adenosine is an important neuromodulator that exerts its functions through interacting with adenosine A_1, A_{2A}, A_{2B}, and A_3 7-transmembrane G-protein coupled receptor (GPCR) subtypes.[6−8] Adenosine A_{2A} receptor is highly expressed in the striatum in central nervous system, where it is colocalized with dopamine D_2 receptors on striatopallisal output neuron.[9] This discrete location limits the risk of unwanted side effects associated with receptors that have broad central nervous system distribution. A number of A_{2A} receptor antagonists have been shown to improve motor disabilities in animal models of Parkinson's disease without inducing dyskinesia.[10] Examples of A_{2A} receptor antagonists that progressed into clinical development are shown in Figure 1.[11,12]

Istradefylline (KW-6002) represents the most advanced A_{2A} receptor antagonist in clinical development.[13,14] It was denied approval in the United States due to questionable balance of risk and benefit.[15] However, on March 25, 2013, Kyowa Hakko received marketing approval of istradefylline under the name of NOURIAST (20 mg orally administrated once daily) in Japan.[16] It represents the world's first antiparkinsonian agent based on antagonizing adenosine A_{2A} receptor. Preladenant was the most advanced nonxanthine A_{2A} antagonist. It is the most potent and selective compound (A_{2A} 1.1 nM, A_1/A_{2A} > 1000) in clinical development.[17] Unfortunately, on May 23, 2013, Merck announced the discontinuation of all development activities of preladenant based on the results of three separate phase III trials, which showed no evidence of efficacy when compared with placebo.[18] The mixed clinical results demonstrate the challenges in pharmaceutical research and development for a complex disease such as Parkinson's disease.

Received: April 5, 2014
Revised: June 11, 2014
Published: June 12, 2014

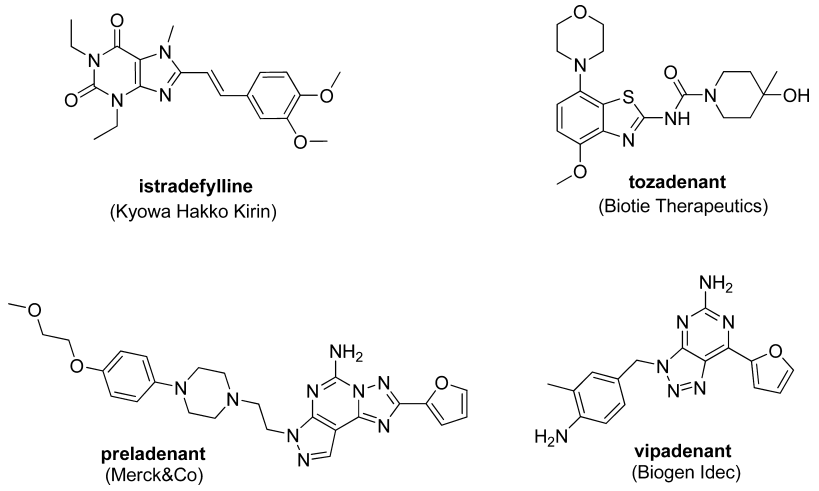

Figure 1. Examples of A_{2A} receptor antagonists in clinical development.

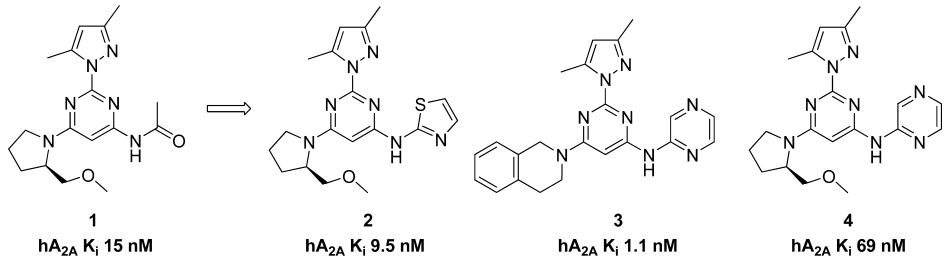

Figure 2. Replacement of acetamide functional group with bioisosteres.

We have focused on 2,4,6-trisubstituted pyrimidines in our pursuit of novel A_{2A} receptor antagonists for the treatment of Parkinson's disease.[19−24] Most recently, we reported a bioisosteric replacement of a potentially labile acetamide functional group. This effort led us to a new series of A_{2A} antagonists, shown in Figure 2, with improved receptor binding affinity and chemical stability.[25] However, when we subjected compound **3** to a preliminary CYP inhibition test, it demonstrated 80% inhibition of CYP3A4 at 10 μM; it also showed inhibition of other CYP isoforms (Table 2). Although these numbers were not particularly worrisome considering the superb receptor binding affinity of compound **3** (1.1 nM), we decided to address this potential problem in our structure−activity relationship (SAR) campaign. Here we report the optimization campaign based on the initial lead compounds aimed at obtaining better receptor binding affinity, ligand efficiency, CYP inhibition profiles, and in vivo efficacy.

RESULTS AND DISCUSSION

Chemistry. The general synthesis of compounds **9**−**23** is outlined in Scheme 1. Commercially available 4,6-dichloro-2-(methylthio)pyrimidine **5** was treated with 2,2,2-trifluoroethylamine in the presence of *N*,*N*-diisopropylethylamine (DIPEA) in *N*-methyl-2-pyrrolidone (NMP) at 100 °C to give **6a**, or reacted with the desired amine in the presence of sodium hexamethyldisilazide (NaHMDS) to give **6b**−**e**. Treatment of **6a**−**e** with oxone produced the corresponding sulfonyl compounds **7a**−**e**, which were reacted with pyrazole in the presence of NaH in tetrahydrofuran (THF) to give intermediates **8a**−**e**. The chlorine atom of the pyrimidine intermediates **8a**−**e** was displaced with (*R*)-2-(methoxymethyl)pyrrolidine hydrochloride in the presence of DIPEA in THF at 50 °C or with 1,2,3,4-tetrahydroisoquinoline in THF at 50 °C, to give the final products **9**−**13** and **14**−**18**, respectively. Treatment of **8a**−**e** with pyrazole in the presence of cesium carbonate in NMP at 95 °C afforded the final compounds **19**−**23**.

Scheme 1. Synthesis of 2,4,6-Trisubstituted Pyrimidines[a]

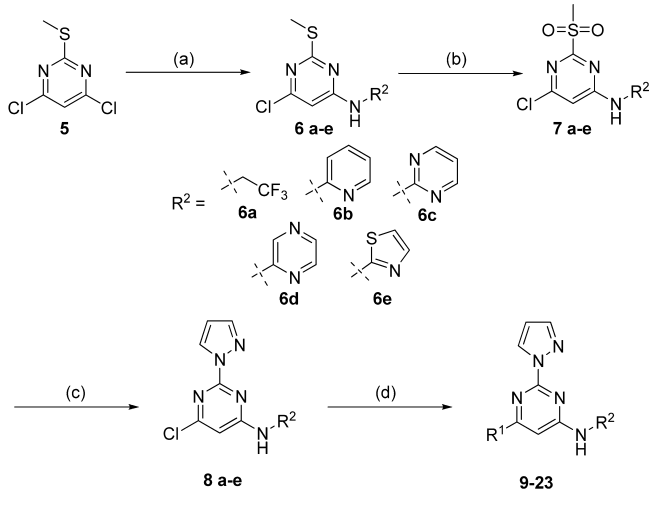

[a]Reagents and conditions: (a) For **6a**: 2,2,2-trifluoroethylamine, DIPEA, NMP, 100 °C, 8 h; for **6b**−**e**: amine, NaHMDS, THF, rt, 8 h. (b) Oxone, THF, H_2O, rt, 10 h. (c) Pyrazole, NaH, THF, rt, 10 h. (d) For **9**−**13**: (*R*)-2-(methoxymethyl)pyrrolidine hydrochloride, DIPEA, THF, 50 °C, 8 h; for **14**−**18**: 1,2,3,4-tetrahydroisoquinoline, THF, 50 °C, 8 h; for **19**−**23**: pyrazole, Cs_2CO_3, NMP, 95 °C, 12 h.

Pharmacology and Structure−Activity Relationship. As mentioned in the introduction, compound **3** demonstrated

dx.doi.org/10.1021/cn5000716 | ACS Chem. Neurosci. 2014, 5, 674−682

Table 1. SAR of Designed Compounds

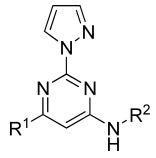

Compd	R^1	R^2	Inhibition [a] (%)	hA_{2A} K_i [b] (nM) ± SEM	clogP [c]	LE [d]
9	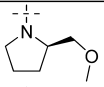		93	2884 ± 633	2.21	0.30
10	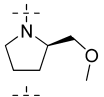		121	0.22 ± 0.13	2.51	0.51
11	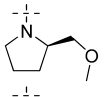		107	181 ± 35	1.59	0.35
12	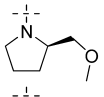		123	55 ± 10	1.83	0.38
13	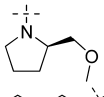		117	577 ± 63	2.47	0.34
14	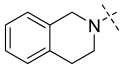		101	928 ± 51	3.22	0.31
15	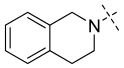		113	0.66 ± 0.17	3.53	0.45
16	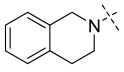		28	ND [e]	2.61	ND
17	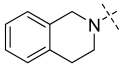		120	330 ± 101	2.85	0.32
18	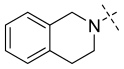		93	771 ± 24	3.48	0.31
19			120	2.16 ± 0.1	1.87	0.54
20			80	ND	2.18	ND
21			86	6945 ± 17	1.26	0.31
22			108	23 ± 0.8	1.50	0.45
23			-53	ND	2.14	ND
	preladenant		120	1.0 ± 0.5	2.35	0.33

[a]The inhibition of [^{3}H]-ZM 241385 binding at human A_{2A} receptors expressed in HEK293 cells at 100 μmol/L concentration. [b]Displacement of [^{3}H]-ZM 241385 binding at human A_{2A} receptors expressed in HEK293 cells. Data are expressed as geometric mean values of at least two runs ± the standard error measurement (SEM). [c]Calculated by Molinspiration. [d]LE (ligand efficiency) = 1.37pK_i/HA (heavy atom). [e]ND = not determined.

80% inhibition of CYP3A4 at 10 μM; it also showed inhibition for other CYP isoforms (Table 2). Although these numbers were not particularly worrisome considering the superb receptor binding affinity of compound **3** (1.1 nM), we decided to address this potential problem in our SAR campaign. We hypothesized that the high lipophilicity might play a role in CYP inhibition. The clogP of compound **3** is 3.29. We set to make the new compounds less lipophilic, and therefore, we chose pyrazole as the substituent of the 2 position of the aminopyrimidine core structure. In addition to the benefit of trimming down one unit of clogP when compared with dimethylpyrazole, pyrazole also demonstrated good potency and metabolic stability in our previous experience.[19] We kept the same set of R^1 and R^2 as in our last exercise[25] for a clear comparison of the SAR.

The SAR of the synthesized compounds is presented in Table 1. With the combination of 2-pyrazole and 4-(*R*)-2-(methoxymethyl) pyrrolidine, the best compound was obtained with pyridine. Compound **10** (0.22 nM) was 5 times more potent than preladenant and, to the best of our knowledge,

dx.doi.org/10.1021/cn5000716 | ACS Chem. Neurosci. 2014, 5, 674−682

represented one of the highest receptor binding affinity of A_{2A} antagonists. Pyrazine was also a reliable bioisostere as compound **12** demonstrated decent activity (55 nM). Pyrimidine, thiazole, and trifluoroethyl all showed diminished activity compared with pyridine and pyrazine (compounds **11**, **13**, and **9**; 181, 577, and 2884 nM, respectively). The trend continued with the combination of 2-pyrazole and 4-tetrahydroisoquinoline, as the best compound also came from pyridine (compound **15**, 0.66 nM). When both 2 and 4 positions were occupied by an aromatic substituent, the best compound was from trifluoroethyl, as compound **19** demonstrated excellent affinity (2.2 nM). Pyrazine, once again, demonstrated decent activity (compound **22**, 23 nM). With the data we obtained so far, among the five bioisosteres evaluated, pyridine and pyrazine proved to be excellent surrogates for acetamide, followed by trifluoroethyl and thiazole, pyrimidine proved to be the least favorable biosiostere for the acetamide. The leading compounds with the highest receptor binding affinity **10**, **15**, and **19** were further profiled in a cell based cAMP assay to confirm them as functional antagonists for the A_{2A} receptor. Compounds **10**, **15**, and **19** demonstrated inhibition of cAMP production (IC_{50} 2.1 ± 0.5, 1.4 ± 0.4, and 0.5 ± 0.3 nM, respectively). Preladenant was tested in the same assay, and its IC_{50} was determined to be 70 ± 7.0 nM. Compounds obtained from this new campaign demonstrated exceptional receptor binding affinity (e.g., compounds **10**, **15**, and **19**, 0.22, 0.66, and 2.2 nM, respectively) and ligand efficiency (e.g., compounds **10**, **15**, and **19**, LE 0.51, 0.45, and 0.54, respectively), with desirable physical-chemical properties (e.g., clogP range from 1.87 for compound **19** to 2.51 for compound **10**). We are currently using modeling tools to understand the structural basis of the observed SAR results with the aid of crystal structures of A_{2A} receptors bound to antagonists and agonists.[26−29]

In Vitro Safety and Potential Drug/Drug Interactions. The reference compounds **3**, **4** and leading compounds **10**, **12** (compound **12** was selected for its decent binding affinity and low clogP), **15**, and **19** were evaluated in a preliminary CYP screening assay to assess their potential liability in liver safety and drug/drug interactions. Compound **3** demonstrated 80% inhibition of CYP3A4 at 10 μM; it also showed inhibition for other CYP isoforms (Table 2). We hypothesized that the high lipophilicity might play a role in CYP inhibition. This assumption was validated as compound **4**, a close analogue to **3**, demonstrated improved CYP profile (except for CYP1A2). Compounds **10** (clogP 2.51), **12** (clogP 1.83), and **19** (clogP 1.87) showed weak CYP3A4 inhibition at 10 μM, while compound **15** (clogP 3.53) demonstrated moderate CYP3A4 inhibition (64%) at 10 μM. Given the exceptional receptor binding affinity of these compounds (e.g., compound **10**, 0.22 nM), we project the potential safety and drug/drug interaction liabilities to be marginal.

Table 2. CYP Inhibition of Designed Compounds

		inhibition (%)				
compd[a]	clogP[b]	CYP3A4	CYP2D6	CYP1A2	CYP2C9	CYP2C19
3	3.29	80	24	64	84	81
4	2.27	52	7	72	69	29
10	2.51	16	18	93	32	36
12	1.83	24	14	95	54	42
15	3.53	64	25	87	65	55
19	1.87	6	16	95	9	8

[a]All compounds were tested at 10 μM concentration. [b]Calculated by Molinspiration.

In Vitro Human and Mouse Liver Microsomal Stability Evaluation. The metabolic stability of compounds **3**, **4**, **10**, **12**, **15**, and **19** was evaluated in human and mouse liver microsomal tests. Under the current experimental conditions, these compounds demonstrated relatively high clearance and short half-lives in both human and mouse liver microsomes. The high clearance was not directly related to the clogP of the tested compounds, as compound **12** (clogP 1.83, MLM Cl_{int} = 132 mL/min/kg, HLM Cl_{int} = 24.7 mL/min/kg) demonstrated lower metabolic stability compared with compound **3** (clogP 3.29, MLM Cl_{int} = 63 mL/min/kg, HLM Cl_{int} = 13.8 mL/min/kg). We had previously obtained metabolic stable compounds using the same substitutions on the aminopyrimidine core,[24] with the exception of the pyridine or pyrazine being replaced by acetamide (e.g., compound **1** and **4**). It was therefore possible that the new compounds with heterocycles as the bioisosteric replacements for the acetamide posted potential metabolic soft spots which accelerated the clearance. However, the unsubstituted pyrazole might also contribute to the high clearance (e.g., compound **19** with trifluoroethyl as the bioisostere for the acetamide).

Table 3. Metabolic Stability of Designed Compounds

	Cl_{int} (mL/min/kg)		$t_{1/2}$ (min)	
compd[a]	HLM[b]	MLM[c]	HLM	MLM
3	13.8	63	51.7	38.3
4	29.2	152	24.4	16
10	57	684	12.6	3.6
12	24.7	132	28.9	18.3
15	56	195	12.6	12.4
19	32	554	22	4.4

[a]All compounds were tested at 1 μM concentration. [b]HLM = human liver microsomes. [c]MLM = mouse liver microsomes.

Haloperidol Induced Catalepsy. We were eager to see if these new compounds could reverse haloperidol induced catalepsy (HIC) in rat to validate the observed in vitro affinity. Because the leading compounds demonstrated fast metabolic clearance, we therefore decided to use intraperitoneal injection (i.p.) route for drug delivery instead of per oral (p.o.) in the HIC to circumvent the first-pass effect in the gastrointestinal tract. KW-6002 5 mg/kg i.p. was used as the standard. Compounds **10**, **15**, and **19** were tested in HIC, and the results are presented in Figure 3. Compounds **10**, **15**, and **19** all demonstrated significant reversal of haloperidol induced catalepsy at all three doses (5, 10, and 30 mg/kg). There was no difference between the doses of 10 and 30 mg/kg, indicating a maximum effective dose having been reached at 10 mg/kg (over 90% reversal). The plasma, brain, and striatum exposures of compound **10** were determined using LC−MS/MS (Table 4). Compound **10** demonstrated proportional exposure in plasma, brain, and striatum in the doses of 10 and 30 mg/kg. Compound **10** readily crossed the blood-brain barrier, with brain/plasma (B/P) ratios ranging from 1.58 to 1.67 for doses of 10 and 30 mg/kg, respectively. Even though we did not determine the unbound drug concentration, the good brain/striatum exposure (232 and 121 ng/g, respectively, for the dose of 10 mg/kg) and the exceptional potency of compound **10** (0.22 nM) warrant the observed efficacy in HIC.

dx.doi.org/10.1021/cn5000716 | ACS Chem. Neurosci. 2014, 5, 674−682

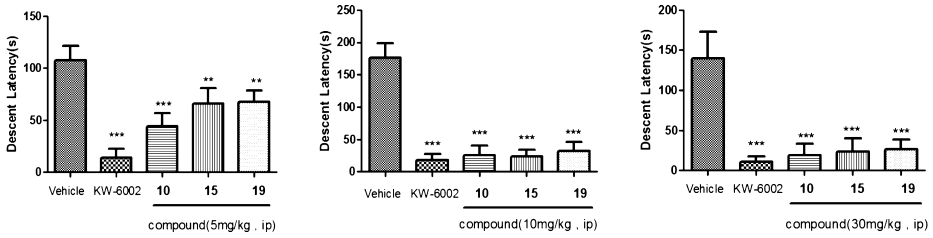

Figure 3. Effect of compounds **10**, **15**, and **19** in the haloperidol induced catalepsy bar test. Mean descent latency (±standard error) in seconds. The vehicle bar represents the mean and standard error from four experiments. KW-6002 was injected (i.p.) in dose of 5 mg/kg. $^{**}p < 0.01$, $^{***}p < 0.001$ versus Vehicle controls.

Table 4. Plasma and Brain Exposure for Compound 10, at 1 h after i.p. Dosing, in Rats Used in the HIC Model

dose (mg/kg)	plasma (ng/mL)[a]	brain (ng/g)[a]	striatum (ng/g)[a]	B/P ratio
10	147 ± 68	232 ± 50	121 ± 88	1.58
30	601 ± 447	1001 ± 550	434[b]	1.67

[a]Data are expressed as geometric mean values of four runs ± the standard error measurement (SEM). [b]Pooled data of four rats.

Summary. We optimized a new series of A_{2A} antagonists based on an aminopyrimidine core. The leading compound **10** demonstrated exceptional receptor binding affinity (hA_{2A} 0.22 nM), ligand efficiency (0.51), and desirable physical-chemical properties (clogP 2.51). Compound **10** showed limited liver safety and drug/drug interaction liabilities. Although the metabolic stability in human and mouse liver microsomes was suboptimal, when dosed i.p., compound **10** readily crossed the blood-brain barrier and demonstrated dose proportional exposures in plasma, brain, and striatum. More importantly, compound **10** exhibited excellent reversal of haloperidol induced catalepsy in rat. Further optimization to improve metabolic stability, as well as molecular modeling to understand the structural basis of the observed SAR are ongoing, and results will be presented in due course.

METHODS

Chemistry. Reaction progress was monitored by analytical thin layer chromatography (TLC) performed on silica gel HSGF254 precoated plates. Organic solutions were dried over anhydrous Na_2SO_4, and the solvents were removed under reduced pressure. ^1H NMR and ^{13}C NMR spectra were obtained on 400 MHz (Varian) spectrometers. Chemical shifts were given in ppm using tetramethylsilane (TMS) as internal standard. Mass spectra were obtained using an Agilent 1100 LC/MSD Trap SL version mass spectrometer. Final compounds were purified with silica gel 100−200 mesh for column chromatography.

*6-Chloro-2-(methylthio)-N-(2,2,2-trifluoroethyl)pyrimidin-4-amine (**6a**).* To a sealed tube were added 4,6-dichloro-2-(methylthio)-pyrimidine (1.95 g, 10 mmol), 2,2,2-trifluoroethanamine (1.98 g, 20 mmol), *N*,*N*-diisopropylethylamine (2.58 g, 20 mmol), and NMP (10 mL). The resulting mixture was heated to 100 °C for 10 h and then poured into H_2O (80 mL). The resulting precipitate was filtered, washed with H_2O (5 mL) and petro ether (5 mL), and dried in vacuum to give a pale yellow solid (1.96 g, 76%). ^1H NMR (400 MHz, $CDCl_3$) δ 6.21 (s, 1H), 5.12 (br s, 1H), 4.22−4.10 (m, 2H), 2.54 (s, 3H).

General Procedure for the Preparation of 6b−e. To a solution of 4,6-dichloro-2-(methylthio)pyrimidine (1.95 g, 10 mmol) and corresponding amine (10 mmol) in THF (15 mL) was added NaHMDS (2 M in THF, 10 mL, 20 mmol) at 0 °C under N_2 atmosphere. The resulting mixture was stirred at room temperature for 8 h and then poured into H_2O (80 mL). The resulting precipitate was filtered, washed with H_2O (5 mL) and petro ether (5 mL), and dried in vacuum to give the title compounds.

*6-Chloro-2-(methylthio)-N-(pyridin-2-yl)pyrimidin-4-amine (**6b**).* Compound **6b** as a pale yellow solid (2.3 g, 91%). ^1H NMR (400 MHz, $CDCl_3$) δ 8.37 (d, J = 4.8 Hz, 1H), 7.71 (dd, J = 4.8 Hz, 1H), 7.61 (s, 1H), 7.47 (s, 1H), 7.42 (d, J = 8.0 Hz, 1H), 7.03 (dd, J = 6.8, 5.4 Hz, 1H), 2.59 (s, 3H).

*N-(6-Chloro-2-(methylthio)pyrimidin-4-yl)pyrimidin-2-amine (**6c**).* Compound **6c** as a pale yellow solid (2.16 g, 85%). ^1H NMR (400 MHz, DMSO-d_6) δ 10.88 (br s, 1H), 8.68 (d, J = 4.4 Hz, 2H), 8.08 (s, 1H), 7.16−7.12 (m, 1H), 7.47 (s, 1H), 2.51 (s, 3H).

*6-Chloro-2-(methylthio)-N-(pyrazin-2-yl)pyrimidin-4-amine (**6d**).* Compound **6d** as a pale yellow solid (2.03 g, 80%). ^1H NMR (400 MHz, $CDCl_3$) δ 8.53 (s, 1H), 8.28 (d, J = 3.6 Hz, 2H), 7.47 (s, 1H), 7.42 (s, 1H), 2.58 (s, 3H).

*N-(6-Chloro-2-(methylthio)pyrimidin-4-yl)thiazol-2-amine (**6e**).* Compound **6e** as a yellow solid (1.97 g, 76%). ^1H NMR (400 MHz, DMSO-d_6) δ 11.95 (br s, 1H), 7.44 (d, J = 2.8 Hz, 1H), 7.22 (d, J = 2.8 Hz, 1H), 6.71 (s, 1H), 2.59 (s, 3H).

General Procedure for the Preparation of 7a−e. To a solution of **6a−e** (6.0 mmol) in THF (15 mL) and H_2O (3 mL) was added oxone (18.0 mmol) at 0 °C. The resulting mixture was stirred at room temperature for 10 h and then poured into H_2O (80 mL). The resulting precipitate was filtered, washed with H_2O (5 mL), and dried in vacuum to give the title compounds, which were used directly in the next step without further purification.

*6-Chloro-2-(methylsulfonyl)-N-(2,2,2-trifluoroethyl)pyrimidin-4-amine (**7a**).* Compound **7a** as a pale yellow solid (1.3 g, 75%).

*6-Chloro-2-(methylsulfonyl)-N-(pyridin-2-yl)pyrimidin-4-amine (**7b**).* Compound **7b** as a pale yellow solid (1.2 g, 70%).

*N-(6-Chloro-2-(methylsulfonyl)pyrimidin-4-yl)pyrimidin-2-amine (**7c**).* Compound **7c** as a pale yellow solid (1.3 g, 76%).

*6-Chloro-2-(methylsulfonyl)-N-(pyrazin-2-yl)pyrimidin-4-amine (**7d**).* Compound **7d** as a pale yellow solid (1.13 g, 66%).

*N-(6-Chloro-2-(methylsulfonyl)pyrimidin-4-yl)thiazol-2-amine (**7e**).* Compound **7e** as an orchid solid (1.64 g, 94%).

General Procedure for the Preparation of 8a−e. To a solution of **7a−e** (4.0 mmol) and 1H-pyrazole (8.0 mmol) in THF (15 mL) was added 80% NaH (8.0 mmol) at 0 °C. The resulting mixture was stirred at room temperature for 10 h, and then poured into H_2O (80 mL). The resulting precipitate was filtered, washed with H_2O (5 mL), and dried in vacuum to give the title compounds.

*6-Chloro-2-(1H-pyrazol-1-yl)-N-(2,2,2-trifluoroethyl)pyrimidin-4-amine (**8a**).* Compound **8a** as a white solid (788 mg, 71%). ^1H NMR (400 MHz, $CDCl_3$) δ 8.51 (s, 1H), 7.80 (s, 1H), 6.47 (s, 1H), 6.40 (s, 1H), 5.58 (br s, 1H), 4.15 (s, 2H).

*6-Chloro-2-(1H-pyrazol-1-yl)-N-(pyridin-2-yl)pyrimidin-4-amine (**8b**).* Compound **8b** as a pale yellow solid (982 mg, 90%). ^1H NMR (400 MHz, $CDCl_3$) δ 8.56 (s, 1H), 8.40 (d, J = 4.0 Hz, 1H), 8.11 (s, 1H), 7.87 (s, 1H), 7.82 (s, 1H), 7.70 (dd, J = 7.6 Hz, 1H), 7.10−6.99 (m, 2H), 6.49 (s, 1H).

*N-(6-Chloro-2-(1H-pyrazol-1-yl)pyrimidin-4-yl)pyrimidin-2-amine (**8c**).* Compound **8c** as a pale yellow solid (927 mg, 85%). ^1H NMR (400 MHz, $CDCl_3$) δ 8.63−8.41 (m, 3H), 7.83 (s, 1H), 7.03−6.99 (m, 1H), 6.50 (s, 1H).

*6-Chloro-N-(pyrazin-2-yl)-2-(1H-pyrazol-1-yl)pyrimidin-4-amine (**8d**).* Compound **8d** as a pale yellow solid (764 mg, 70%). ^1H NMR

dx.doi.org/10.1021/cn5000716 | ACS Chem. Neurosci. 2014, 5, 674−682

(400 MHz, $CDCl_3$) δ 8.57 (d, J = 2.8 Hz, 1H), 8.55 (s, 1H), 8.34 (s, 1H), 8.30 (d, J = 2.8 Hz, 1H), 8.06 (s, 1H), 8.00 (s, 1H), 7.84 (s, 1H), 6.51 (s, 1H).

*N-(6-Chloro-2-(1H-pyrazol-1-yl)pyrimidin-4-yl)thiazol-2-amine (**8e**).* Compound **8e** as a pale yellow solid (763 mg, 71%). ^{1}H NMR (400 MHz, DMSO-d_6) δ 8.71 (s, 1H), 7.92 (s, 1H), 7.53 (d, J = 2.8 Hz, 1H), 7.33 (d, J = 2.8 Hz, 1H), 6.95 (br s, 1H), 6.67 (s, 1H).

General Procedure for the Preparation of 9−13. To a solution of **8a−e** (0.3 mmol) and (*R*)-2-(methoxymethyl)pyrrolidine hydrochloride (0.6 mmol) in THF (1 mL) was added *N*,*N*-diisopropylethylamine (1.2 mmol). The resulting mixture was stirred at 50 °C for 8 h.

*(R)-6-(2-(Methoxymethyl)pyrrolidin-1-yl)-2-(1H-pyrazol-1-yl)-N-(2,2,2-trifluoroethyl)pyrimidin-4-amine (**9**).* The reaction mixture was poured into H_2O (10 mL), and the resulting precipitate was filtered, washed with H_2O (2 mL) and petro ether (2 mL), and dried in vacuum to give the title compound (53 mg, 50%) as a pale yellow solid. ^{1}H NMR (400 MHz, $CDCl_3$) δ 8.49 (s, 1H), 7.74 (s, 1H), 6.41 (s, 1H), 5.45−5.20 (m, 2H), 4.52−4.25 (m, 1H), 4.12−3.88 (m, 2H), 3.75−3.30 (m, 4H), 3.35 (s, 3H), 2.15−1.92 (m, 4H). LCMS (ESI): m/z 356.9.

*(R)-6-(2-(Methoxymethyl)pyrrolidin-1-yl)-2-(1H-pyrazol-1-yl)-N-(pyridin-2-yl)pyrimidin-4-amine (**10**).* The reaction mixture was poured into H_2O (10 mL), and the resulting mixture was extracted with ethyl acetate (10 mL × 3), dried over Na_2SO_4, and concentrated. The residue was purified by flash chromatography (0.5% MeOH/CH_2Cl_2) to give the title compound (81 mg, 77%) as a pale yellow solid. ^{1}H NMR (400 MHz, $CDCl_3$) δ 8.56 (d, J = 2.0 Hz, 1H), 8.33 (d, J = 4.4 Hz, 1H), 7.79 (s, 1H), 7.65−7.61 (m, 1H), 7.49 (s, 1H), 7.29 (br s, 1H), 6.99 (d, J = 4.4 Hz, 1H), 6.93−6.89 (m, 1H), 6.45 (s, 1H), 4.51−4.49 (m, 1H), 3.72−3.65 (m, 3H), 3.45 (s, 3H), 3.42 (s, 1H), 2.15−2.06 (m, 4H). ^{13}C NMR (100 MHz, $CDCl_3$) δ 162.3, 158.8, 154.6, 153.7, 147.7, 142.4, 137.8, 128.7, 116.8, 112.3, 107.4, 84.9, 77.2, 72.4, 59.2, 57.1, 47.3. HRMS (ESI) calcd for $C_{18}H_{21}N_7O$ $(M + H)^+$, 352.1880; found, 352.1878.

*(R)-N-(6-(2-(Methoxymethyl)pyrrolidin-1-yl)-2-(1H-pyrazol-1-yl)-pyrimidin-4-yl)pyrimidin-2-amine (**11**).* The reaction mixture was poured into H_2O (10 mL), and the resulting precipitate was filtered, washed with H_2O (2 mL) and petro ether (2 mL), and dried in vacuum to give the title compound (26 mg, 25%) as a pale yellow solid. ^{1}H NMR (400 MHz, $CDCl_3$) δ 8.53 (s, 3H), 8.16 (s, 1H), 7.77 (s, 1H), 7.43 (br s, 1H), 6.87−6.85 (m, 1H), 6.43 (s, 1H), 4.60−4.44 (m, 1H), 3.69−3.48 (m, 3H), 3.42 (s, 3H), 2.20−1.96 (m, 4H). LCMS (ESI): m/z 352.9.

*(R)-6-(2-(Methoxymethyl)pyrrolidin-1-yl)-N-(pyrazin-2-yl)-2-(1H-pyrazol-1-yl)pyrimidin-4-amine (**12**).* The reaction mixture was poured into H_2O (10 mL), and the resulting mixture was extracted with ethyl acetate (10 mL × 3), dried over Na_2SO_4, and concentrated. The residue was purified by flash chromatography (0.5% MeOH/CH_2Cl_2) to give the title compound (50 mg, 47%) as a pale yellow solid. ^{1}H NMR (400 MHz, $CDCl_3$) δ 8.53 (s, 1H), 8.39 (s, 1H), 8.22 (s, 1H), 8.14 (d, J = 2.0 Hz, 1H), 7.78 (s, 1H), 7.10 (br s, 1H), 6.44 (s, 1H), 4.62−4.48 (m, 1H), 3.75−3.53 (m, 3H), 3.50−3.42 (m, 1H), 3.42 (s, 3H), 2.22−2.00 (m, 4H). ^{13}C NMR (100 MHz, $CDCl_3$) δ 162.4, 158.2, 154.7, 150.4, 142.6, 141.3, 136.4, 135.7, 128.8, 107.6, 85.5, 77.2, 72.4, 59.2, 57.3, 47.4. HRMS (ESI) calcd for $C_{17}H_{20}N_8O$ $(M + H)^+$, 353.1833; found, 353.1830.

*(R)-N-(6-(2-(Methoxymethyl)pyrrolidin-1-yl)-2-(1H-pyrazol-1-yl)-pyrimidin-4-yl)thiazol-2-amine (**13**).* The reaction mixture was poured into H_2O (10 mL), and the resulting precipitate was filtered, washed with H_2O (2 mL) and petro ether (2 mL), and dried in vacuum to give the title compound (24 mg, 22%) as a pale yellow solid. ^{1}H NMR (400 MHz, $CDCl_3$) δ 8.70 (s, 1H), 7.85 (s, 1H), 7.49 (d, J = 3.2 Hz, 1H), 6.96 (d, J = 3.2 Hz, 1H), 6.49 (s, 1H), 5.96 (br s, 1H), 4.68−4.55 (m, 1H), 3.80−3.43 (m, 4H), 3.42 (s, 3H), 2.25−2.00 (m, 4H). LCMS (ESI): m/z 357.8.

General Procedure for the Preparation of 14−18. To a solution of **8a−e** (0.3 mmol) in THF (1 mL) was added 1,2,3,4-tetrahydroisoquinoline (0.9 mmol). The resulting mixture was stirred at 50 °C for 8 h.

*6-(3,4-Dihydroisoquinolin-2(1H)-yl)-2-(1H-pyrazol-1-yl)-N-(2,2,2-trifluoroethyl)pyrimidin-4-amine (**14**).* The reaction mixture was poured into H_2O (10 mL), and the resulting mixture was extracted with ethyl acetate (10 mL × 3), dried over Na_2SO_4, and concentrated. The residue was purified by flash chromatography (0.5% MeOH/CH_2Cl_2) to give the title compound (57 mg, 51%) as a pale yellow solid. ^{1}H NMR (400 MHz, $CDCl_3$) δ 8.57 (s, 1H), 7.74 (s, 1H), 7.27−7.23 (m, 4H), 6.43 (s, 1H), 5.49 (s, 1H), 5.25 (br s, 1H), 4.76 (s, 2H), 4.09−4.07 (m, 2H), 3.94−3.92 (m, 2H), 2.98−2.97 (m, 2H). LCMS (ESI): m/z 374.9.

*6-(3,4-Dihydroisoquinolin-2(1H)-yl)-2-(1H-pyrazol-1-yl)-N-(pyridin-2-yl)pyrimidin-4-amine (**15**).* The reaction mixture was poured into H_2O (10 mL), and the resulting mixture was extracted with ethyl acetate (10 mL × 3), dried over Na_2SO_4, and concentrated. The residue was purified by flash chromatography (0.5% MeOH/CH_2Cl_2) to give the title compound (35 mg, 32%) as a pale yellow solid. ^{1}H NMR (400 MHz, $CDCl_3$) δ 8.60 (dd, J = 2.6, 0.6 Hz, 1H), 8.36 (dd, J = 5.0, 1.2 Hz, 1H), 7.78 (dd, J = 1.5, 0.7 Hz, 1H), 7.66−7.57 (m, 2H), 7.34 (s, 1H), 7.26−7.18 (m, 4H), 7.04 (d, J = 8.3 Hz, 1H), 6.91 (ddd, J = 7.2, 5.0, 0.8 Hz, 1H), 6.45 (dd, J = 2.6, 1.6 Hz, 1H), 4.84 (s, 2H), 3.98 (s, 2H), 3.00 (t, J = 5.9 Hz, 2H). LCMS (ESI): m/z 369.9.

*N-(6-(3,4-Dihydroisoquinolin-2(1H)-yl)-2-(1H-pyrazol-1-yl)-pyrimidin-4-yl)pyrimidin-2-amine (**16**).* The reaction mixture was poured into H_2O (10 mL), and the resulting precipitate was filtered, washed with H_2O (2 mL) and petro ether (2 mL), and dried in vacuum to give the title compound (38 mg, 34%) as a pale yellow solid. ^{1}H NMR (400 MHz, $CDCl_3$) δ 8.63 (s, 1H), 8.60 (d, J = 4.7 Hz, 2H), 8.14 (s, 1H), 7.82 (s, 1H), 7.71 (s, 1H), 7.29−7.26 (m, 4H), 6.96−6.91 (m, 1H), 6.49 (s, 1H), 4.91 (s, 2H), 4.04 (s, 2H), 3.05 (t, J = 5.6 Hz, 2H). LCMS (ESI): m/z 370.9.

*6-(3,4-Dihydroisoquinolin-2(1H)-yl)-N-(pyrazin-2-yl)-2-(1H-pyrazol-1-yl)pyrimidin-4-amine (**17**).* The reaction mixture was poured into H_2O (10 mL), and the resulting mixture was extracted with ethyl acetate (10 mL × 3), dried over Na_2SO_4, and concentrated. The residue was purified by flash chromatography (0.5% MeOH/CH_2Cl_2) to give the title compound (49 mg, 44%) as a pale yellow solid. ^{1}H NMR (400 MHz, $CDCl_3$) δ 8.61 (d, J = 2.0 Hz, 1H), 8.50 (s, 1H), 8.29 (s, 1H), 8.17 (d, J = 2.0 Hz, 1H), 7.81 (s, 1H), 7.75 (s, 1H), 7.30−7.23 (m, 4H), 6.47 (s, 1H), 4.86 (s, 2H), 3.99 (s, 2H), 3.03 (t, J = 5.9 Hz, 2H). LCMS (ESI): m/z 370.9.

*N-(6-(3,4-Dihydroisoquinolin-2(1H)-yl)-2-(1H-pyrazol-1-yl)-pyrimidin-4-yl)thiazol-2-amine (**18**).* The reaction mixture was poured into H_2O (10 mL), and the resulting precipitate was filtered, washed with H_2O (2 mL) and petro ether (2 mL), and dried in vacuum to give the title compound (25 mg, 22%) as a pale yellow solid. ^{1}H NMR (400 MHz, $CDCl_3$) δ 8.86 (s, 1H), 7.86 (s, 1H), 7.48 (s, 1H), 7.25−7.22 (m, 4H), 6.97 (s, 1H), 6.51 (s, 1H), 6.05 (s, 1H), 4.81 (s, 2H), 3.99−3.97 (m, 2H), 3.01−3.00 (m, 2H). LCMS (ESI): m/z 375.8.

General Procedure for the Preparation of 19−23. To a sealed tube was added **8a−e** (0.3 mmol), 1*H*-pyrazole (1.2 mmol), Cs_2CO_3 (0.9 mmol), and NMP (1 mL). The resulting mixture was stirred at 95 °C for 12 h.

*2,6-Di(1H-pyrazol-1-yl)-N-(2,2,2-trifluoroethyl)pyrimidin-4-amine (**19**).* The reaction mixture was poured into H_2O (10 mL), and the resulting precipitate was filtered, washed with H_2O (2 mL) and petro ether (2 mL), and dried in vacuum to give the title compound (21 mg, 23%) as a pale yellow solid. ^{1}H NMR (400 MHz, $CDCl_3$) δ 8.66 (s, 1H), 8.58 (d, J = 2.0 Hz, 1H), 7.84 (s, 1H), 7.78 (s, 1H), 7.00 (s, 1H), 6.50 (s, 2H), 5.68 (br s, 1H), 4.20−4.18 (m, 2H). ^{13}C NMR (100 MHz, $CDCl_3$) δ 164.9, 158.4, 155.2, 143.6, 143.5, 129.5, 128.3, 124.2 (q, J = 254.3 Hz), 108.5, 108.4, 77.2, 30.8 (q, J = 53.7 Hz). HRMS (ESI) calcd for $C_{12}H_{10}F_3N_7$ $(M + Na)^+$, 332.0842; found, 332.0840.

*2,6-Di(1H-pyrazol-1-yl)-N-(pyridin-2-yl)pyrimidin-4-amine (**20**).* The reaction mixture was poured into H_2O (10 mL), and the resulting mixture was extracted with ethyl acetate (10 mL × 3), dried over Na_2SO_4, and concentrated. The residue was purified by flash chromatography (0.5% MeOH/CH_2Cl_2) to give the title compound (23 mg, 25%) as a pale yellow solid. ^{1}H NMR (400 MHz, $CDCl_3$) δ 8.66 (d, J = 2.0 Hz, 1H), 8.63 (s, 1H), 8.45 (d, J = 4.4 Hz, 1H), 8.36

dx.doi.org/10.1021/cn5000716 | ACS Chem. Neurosci. 2014, 5, 674−682

(s, 1H), 7.91 (br s, 1H), 7.86 (s, 1H), 7.84 (s, 1H), 7.74−7.70 (m, 1H), 7.32 (d, J = 8.0 Hz, 1H), 7.04−7.01 (m, 1H), 6.53 (s, 2H). LCMS (ESI): m/z 304.9.

*N-(2,6-Di(1H-pyrazol-1-yl)pyrimidin-4-yl)pyrimidin-2-amine (**21**).* The reaction mixture was poured into H_2O (10 mL), and the resulting precipitate was filtered, washed with H_2O (2 mL) and petro ether (2 mL), and dried in vacuum to give the title compound (29 mg, 32%) as a pale yellow solid. ^{1}H NMR (400 MHz, $CDCl_3$) δ 8.92 (s, 1H), 8.69 (s, 2H), 8.68 (s, 1H), 8.63 (s, 1H), 8.56 (s, 1H), 7.86 (s, 2H), 6.99 (s, 1H), 6.54 (s, 2H). LCMS (ESI): m/z 305.9.

*N-(Pyrazin-2-yl)-2,6-di(1H-pyrazol-1-yl)pyrimidin-4-amine (**22**).* The reaction mixture was poured into H_2O (10 mL), and the resulting precipitate was filtered, washed with H_2O (2 mL) and petro ether (2 mL), and dried in vacuum to give the title compound (25 mg, 27%) as a pale yellow solid. ^{1}H NMR (400 MHz, $CDCl_3$) δ 8.75 (s, 1H), 8.67 (d, J = 1.8 Hz, 1H), 8.63 (d, J = 1.8 Hz, 1H), 8.38 (s, 2H), 8.29 (d, J = 1.8 Hz, 1H), 8.08 (s, 1H), 7.88 (s, 1H), 7.85 (s, 1H), 6.54 (s, 2H). LCMS (ESI): m/z 305.9.

*N-(2,6-Di(1H-pyrazol-1-yl)pyrimidin-4-yl)thiazol-2-amine (**23**).* The reaction mixture was poured into H_2O (10 mL), and the resulting precipitate was filtered, washed with H_2O (2 mL) and petro ether (2 mL), and dried in vacuum to give the title compound (55 mg, 51%) as a pale yellow solid. ^{1}H NMR (400 MHz, DMSO-d_6) δ 12.21 (s, 1H), 8.92 (s, 1H), 8.81 (s, 1H), 7.95 (s, 2H), 7.52 (s, 1H), 7.39 (br s, 1H), 7.31 (s, 1H), 6.67 (s, 2H). LCMS (ESI): m/z 310.8.

Cell Culture. HEK293 cells stably expressing human A_{2A} (HEK 293-A_{2A} cells) were obtained from Academy of Military Medical Sciences (Beijing China). The cells were cultured in DF12 supplemented with 10% fetal bovine serum (FBS), 1% penicillin, streptomycin, and 400 μg/mL G418. The cells were maintained at 37 °C in an incubator under a humidified atmosphere of 95% air and 5% CO_2.

Membrane Preparation. Cultured cells in 10 × 10 cm dishes were washed by ice-cold phosphate-buffered saline (PBS) once and then scraped into an EP tube. They were then collected by using the 4 °C centrifuge with the lysis buffer containing 5 mM Tris-HCl pH 7.4, 5 mM EDTA·2Na, and 5 mM EGTA in the presence of PMSF (1:1000) and incubated for 30 min on ice with extraction by using a 1 mL needle for 15 times. After centrifugation at 40 000g for 20 min, the supernatant was discarded. Pellets were resuspended in reaction buffer (50 mM Tris-HCl pH 7.4, 2 mM $MgCl_2$) with mechanical extraction by using a 1 mL needle for 15 times and then centrifuged at 40 000g for 20 min. The final pellets were suspended in reaction buffer with mechanical extraction. The aliquot of membranes were frozen at −80 °C.

Radioligand Binding Assay. An aliquot of membranes (50−100 μg of protein) was treated with adenosine deaminase (2 U/mL, type X bovine spleen, Sigma) and incubated at 37 °C for 30 min with 1.0 nM [^{3}H]-ZM 241385 (50.00 Ci/mmol ART 0884) for the A_{2A} human membranes in the presence of varying concentrations of competing ligand. Nonspecific binding was determined in the presence of 10 μM NECA for A_{2A} membranes. Incubation was terminated by rapid filtration over 12-well filter plate (Millipore) equipped with GF/B filter papers (Whatman, U.K.). Filters were washed three times with ice-cold 50 mM Tris-HCl buffer. The filter papers, after being oven-dried, were incubated with a scintillation cocktail (methylbenzene 500 mL, POPOP 50 mg, PPO 2 g), and radioactivity was counted on a Beckman LS-6500 (PerkinElmer) counter. Binding data were fitted in one-site competition binding model for IC_{50} determination, performed with GraphPad Prism (GraphPad Software, San Diego, CA), and K_i values were calculated based on the Cheng-Prusoff equation (K_i = $IC_{50}/(1 + (L/K_d))$).

cAMP Functional Assay. HEK-293 cells transfected with A_{2A} receptor were used. All cells were cultured in DMEM-F12 nutrient mixture supplemented with 10% FBS, 0.05% Geneticin, 1% penicillin, and 1% streptomycin at 37 °C in 5% CO_2. The cells were detached with 0.25% trypsin solution (0.25% trypsin). The cells were collected at 1100r/min for 3 min at room temperature and resuspended in Hank's balanced salt solution (138 mM NaCl, 5 mM KCl, 1.3 mM $CaCl_2$, 0.5 mM $MgCl_2$, 0.4 mM $MgSO_4$, 0.3 mM KH_2PO_4, 0.3 mM Na_2HPO_4, 5.6 mM glucose, pH 7.4) containing 100 μM 3-isobutyl-1-methylxanthine (Sigma, I7018) as phosphodiesterase inhibitor. The cells were loaded into 384-well plates (~4000 cells/well) and incubated with test compound (10^{-4}−10^{-11} M) for 90 min at 37 °C, and then the A_{2A} receptor agonist NECA (1 μM final concentration) was added to the sample and the mixture was incubated again for 10 min at room temperature. The cAMP production was measured by using a Cisbio kit according to the manufacturer's instructions. Briefly, the fluorescence signals at 665 and 620 nm were measured and the ratio was determined. The cyclic AMP levels were calculated according to the corresponding standard curve. IC_{50} values were obtained from concentration−response curves after log transformation.

Catalepsy. Haloperidol (1.5 mg/kg) and KW-6002 (5 mg/kg) and compounds (30 mg/kg, 10 mg/kg, 5 mg/kg) were dissolved in 5% DMSO, 5% Tween 80, 5% cremophor, and 85% saline. Male Wistar (about 220 g) rats were habituated to the vivarium for 1 week prior to testing. Animals (n = 4/total N = 20) were randomly assigned to different groups, and behavioral testing was performed blindly to each group. The data about different dosages were collected once a week to allow for complete drug washout during testing sessions. One hour prior to testing, the animals were intraperitoneally (i.p.) injected with KW-6002 or compounds, followed by injection of haloperidol (i.p.) 30 min before the testing. The behavioral test trial (maximum duration of 200 s) began by placing the forepaws of rats on a 10 cm high bar (horizontally placed) and hind quarters on a platform. Time was recorded when the animal fully removed both paws from the bar or climbed onto the bar with all of its limbs. After the haloperidol-induced catalepsy test (samples collected about 1 h), the plasma and brain were collected for the preclinical assays.

Assessment of Metabolic Stability in Liver Microsomes. To evaluate metabolic stability in vitro, test compounds were incubated with mouse and human liver microsomes in the presence of NADPH (in triplicate). The reaction mixture consisted of microsomes (0.2 mg/mL), phosphate buffer (100 mM, pH 7.4), NADPH (1 mM), and test compounds (1 μM). Prior to the start of the incubation, the mixture was warmed up at 37 °C for 5 min. The reaction was initiated by the addition of NADPH to a final concentration of 1 mM. Aliquots of 50 μL samples were taken at six time points (0, 10, 20, 30, 45, and 60 min), and then placed into Eppendorf tubes containing 100 μL of cold acetonitrile with internal standard. Samples were then centrifuged at 13 000 rpm for 10 min, and an aliquot of 10 μL of the supernatants was subject to LC−MS/MS analysis. Substrate depletion parameters were calculated using the following equations:

$$t_{1/2} = \frac{0.693}{k} \tag{1}$$

where k is the slope from the linear regression analysis of the ln[% remaining] of test compound as a function of incubation time.

$$\mathrm{Cl}_{\mathrm{int,in\ vitro}} = \frac{k}{\text{mg of protein per mL incubation}} \times \frac{\text{mg of protein}^{a}}{\text{g of liver}} \times \frac{\text{g of liver}}{\text{kg of body weight}}^{b} \tag{2}$$

where a is 20 mg/g for mouse and human, and b is 87.5 g/kg for mouse and 25.7 g/kg for human.[30]

$$\mathrm{Cl}_{\mathrm{hepatic}} = \frac{\mathrm{Cl}_{\mathrm{int,in\ vitro}} Q_h}{\mathrm{Cl}_{\mathrm{int,in\ vitro}} + Q_h} \tag{3}$$

where Q_h is the hepatic blood flow (90 mL/min for mouse and 20.7 mL/min for human).

Evaluation of CYP Inhibitory Potency. Inhibitory potency of test compounds against human P450 enzymes was investigated in human liver microsomes. The five major CYP isoforms and their respective probe substrates were as follows: CYP1A2 (phenacetin, 30 μM), CYP2C9 (tolutamide, 100 μM), CYP2C19 (S-mephenytoin, 40 μM), CYP2D6 (dextromethorphan, 5 μM), and CYP3A4 (midazolam, 1 μM). All probe substrates were used at concentrations near or below

dx.doi.org/10.1021/cn5000716 | ACS Chem. Neurosci. 2014, 5, 674−682

their K_ms (Michaelis constant). Triplicate incubations were conducted in the 200 μL incubation mixtures at 37 °C. The mixture contained HLM (0.2 mg/mL), phosphate buffer (100 mM, pH 7.4), NADPH (1 mM), tested compounds (10 μM), and individual CYP probe substrate. The mixtures were preincubated for 10 min to allow inhibitor/enzyme interactions before the initiation of the reaction with NADPH. After a specific time period (10 min for CYP1A2, 2D6 and 3A4; 30 min for CYP2C9 and 2C19), reactions were terminated by the addition of 100 μL of cold acetonitrile containing an appropriate internal standard. Samples were then centrifuged and injected into the LC−MS/MS apparatus to quantify the concentrations of specific metabolites formed by individual CYP enzymes.

LC−MS/MS Analysis. All samples were analyzed by using a LC−MS/MS system consisting of an API4000 Qtrap mass spectrometer equipped with a turbo-V ionization source (Applied Biosystems, Ontatrio, Canada), two LC-20AD pumps with a CBM-20A controller, DGU-20A solvent degasser, and a SIL-20A autosampler (Shimadzu, Columbia, MD). An Agela Venusil XBP C18 column (50 × 2.1 mm; 5 μm particle size) was used to achieve HPLC separation. Column temperature was held at 40 °C. Flow rate was 0.3 mL/min with the total run time of 6 min.

For MS/MS quantitation, the API4000 Qtrap mass spectrometer was operated in the ESI positive mode with multiple reaction-monitoring (MRM). All compounds and the internal standard were monitored with dwell time set to 100 ms. Other MS/MS parameters were set as follows: curtain gas, 30 psi; nebulizer gas (GS1), 55 psi; turbo gas (GS2), 55 psi; ion spray voltage, 4500 V; and ion source temperature, 500 °C. For the selected ion transitions, the declustering potential (DP) and the collision energy (CE) were optimized for the best sensitivity for each analyte. Data were collected and processed using AB Sciex Analysist 1.5.2 data collection and integration software.

■ ASSOCIATED CONTENT

Supporting Information

^1H and ^{13}C NMR files of synthetic intermediates and final products as described in the text. This material is available free of charge via the Internet at http://pubs.acs.org.

■ AUTHOR INFORMATION

Corresponding Authors

*(X.H.Z.) Mailing address: Soochow University College of Pharmaceutical Sciences, 199 Ren Ai Road, Suzhou, Jiangsu, P.R.China 215123. E-mail: xiaohuzhang@suda.edu.cn. Telephone: (86)512 65880380. Fax: (86)512 65880380.

*(X.C.Z.) Mailing address: Soochow University College of Pharmaceutical Sciences, 199 Ren Ai Road, Suzhou, Jiangsu, P.R.China 215123. E-mail: zhenxuechu@suda.edu.cn. Telephone: (86)512 65880369. Fax: (86)512 65880369.

Author Contributions

†J.Z. and Z.Y.contributed equally to this paper. X.H.Z. conceived the project, and oversaw and designed the chemistry. J.Z., Z.Y., and H.M. performed synthetic chemistry work. M.W. and H.Z. performed and interpreted in vitro DMPK experiments. X.L. and L.L. performed the pharmacology and in vivo experiments, and X.C.Z. interpreted the data.

Funding

This work was supported by National Natural Science Foundation of China (Grant No. 81273372, 81130023, 31373382); National Basic Research Plan (973) of the Ministry of Science and Technology of China (2011CB5C4403); China Postdoctoral Science Foundation (2013M541729), BM2013003, and PAPD (A Project Funded by the Priority Academic Program Development of Jiangsu Higher Education Institutions).

Notes

The authors declare no competing financial interest.

■ ABBREVIATIONS

B/P, brain/plasma; CE, collision energy; DIPEA, *N*,*N*-diisopropylethylamine; DMSO, dimethyl sulfoxide; L-Dopa, levodopa; DP, declustering potential; EDTA·2Na, ethylenediaminetetraacetic acid disodium salt; EGTA, ethylene glycol-bis(2-aminoethyl ether)-*N*,*N*,*N*′,*N*′-tetraacetic acid; FBS, fetal bovine serum; GPCR, G protein-coupled receptor; HA, heavy atom; HIC, haloperidol induced catalepsy; HLM, human liver microsomes; i.p., intraperitoneal injection; LE, ligand efficiency; MLM, mouse liver microsomes; MRM, multiple reaction-monitoring; NADPH, reduced nicotinamide adenine dinucleotide phosphate; NaHMDS, sodium hexamethyldisilazide; ND, not determined; NECA, 5′-(*N*-ethylcarboxamido)adenosine; NMP, *N*-methyl-2-pyrrolidone; PBS, phosphate-buffered saline; PMSF, phenylmethanesulfonyl fluoride; p.o., per oral; POPOP, bis(phenyloxazolyl) benzene; PPO, 2,5-diphenyloxazole; SAR, structure−activity relationship; SEM, standard error of the mean; THF, tetrahydrofuran; Tris-HCl, tris(2-carboxyethyl)phosphine hydrochloride

■ REFERENCES

(1) Lees, A. J., Hardy, J., and Revesz, T. (2009) Parkinson's disease. *Lancet 373*, 2055−2066.

(2) Dorsey, E., Constantinescu, R., Thompson, J., Biglan, K., Holloway, R., Kieburtz, K., Marshall, F., Ravina, B., Schifitto, G., and Siderowf, A. (2007) Projected number of people with Parkinson disease in the most populous nations, 2005 through 2030. *Neurology 68*, 384−386.

(3) Ahlskog, J. E., and Muenter, M. D. (2001) Frequency of levodopa-related dyskinesias and motor fluctuations as estimated from the cumulative literature. *Mov. Disord. 16*, 448−458.

(4) Rascol, O., Brooks, D. J., Korczyn, A. D., De Deyn, P. P., Clarke, C. E., and Lang, A. E. (2000) A five-year study of the incidence of dyskinesia in patients with early Parkinson's disease who were treated with ropinirole or levodopa. *N. Engl. J. Med. 342*, 1484−1491.

(5) Chaudhuri, K., and Schapira, A. H. (2009) Non-motor symptoms of Parkinson's disease: dopaminergic pathophysiology and treatment. *Lancet Neurol. 8*, 464−474.

(6) Ralevic, V., and Burnstock, G. (1998) Receptors for purines and pyrimidines. *Pharmacol. Rev. 50*, 413−492.

(7) Fredholm, B. B., AP, I. J., Jacobson, K. A., Klotz, K. N., and Linden, J. (2001) International Union of Pharmacology. XXV. Nomenclature and classification of adenosine receptors. *Pharmacol. Rev. 53*, 527−552.

(8) Fredholm, B. B., Abbracchio, M. P., Burnstock, G., Daly, J. W., Harden, T. K., Jacobson, K. A., Leff, P., and Williams, M. (1994) Nomenclature and classification of purinoceptors. *Pharmacol. Rev. 46*, 143−156.

(9) Svenningsson, P., Le Moine, C., Fisone, G., and Fredholm, B. B. (1999) Distribution, biochemistry and function of striatal adenosine A_{2A} receptors. *Prog. Neurobiol. 59*, 355−396.

(10) Fredduzzi, S., Moratalla, R., Monopoli, A., Cuellar, B., Xu, K., Ongini, E., Impagnatiello, F., Schwarzschild, M. A., and Chen, J. F. (2002) Persistent behavioral sensitization to chronic L-DOPA requires A_{2A} adenosine receptors. *J. Neurosci. 22*, 1054−1062.

(11) Suzuki, F. S., and Shimada, J. (2000) *Adenosine Antagonist and Parkinson's Disease* (Kase, H., Richardson, P. J., and Jenner, P., Eds.); Academic Press: New York; pp 31−43.

(12) Shah, U., and Hodgson, R. (2010) Recent progress in the discovery of adenosine A_{2A} receptor antagonists for the treatment of Parkinson's disease. *Curr. Opin. Drug Discovery Dev. 13*, 466−480.

(13) Jenner, P. (2005) Istradefylline, a novel adenosine A_{2A} receptor antagonist, for the treatment of Parkinson's disease. *Expert Opin. Invest. Drugs 14*, 729−738.
(14) Jenner, P., Mori, A., Hauser, R., Morelli, M., Fredholm, B. B., and Chen, J. F. (2009) Adenosine, adenosine A_{2A} antagonists, and Parkinson's disease. *Parkinsonism Relat. Disord. 15*, 406−413.
(15) Kyowa Hakko receives not approvable letter from FDA for Istradefylline (KW-6002), *Kyowa Hakko Kirin Co Ltd Press Release,* February 28, 2008.
(16) Approval for manufacturing and marketing of NOURIAST® tablets 20 mg, a novel antiparkinsonian agent, *Kyowa Hakko Kirin Co Ltd Press Release,* March 25, 2013.
(17) Neustadt, B. R., Hao, J., Lindo, N., Greenlee, W. J., Stamford, A. W., Tulshian, D., Ongini, E., Hunter, J., Monopoli, A., Bertorelli, R., Foster, C., Arik, L., Lachowicz, J., Ng, K., and Feng, K. I. (2007) Potent, selective, and orally active adenosine A_{2A} receptor antagonists: arylpiperazine derivatives of pyrazolo[4,3-e]-1,2,4-triazolo[1,5-c]-pyrimidines. *Bioorg. Med. Chem. Lett. 17*, 1376−1380.
(18) Merck provides update on phase III clinical program for Preladenant, the company's investigational Parkinson's disease medicine, *Merck Press Release,* May 23, 2013.
(19) Slee, D. H., Zhang, X., Moorjani, M., Lin, E., Lanier, M. C., Chen, Y., Rueter, J. K., Lechner, S. M., Markison, S., Malany, S., Joswig, T., Santos, M., Gross, R. S., Williams, J. P., Castro-Palomino, J. C., Crespo, M. I., Prat, M., Gual, S., Diaz, J. L., Wen, J., O'Brien, Z., and Saunders, J. (2008) Identification of novel, water-soluble, 2-amino-N-pyrimidin-4-yl acetamides as A_{2A} receptor antagonists with in vivo efficacy. *J. Med. Chem. 51*, 400−406.
(20) Slee, D. H., Chen, Y., Zhang, X., Moorjani, M., Lanier, M. C., Lin, E., Rueter, J. K., Williams, J. P., Lechner, S. M., Markison, S., Malany, S., Santos, M., Gross, R. S., Jalali, K., Sai, Y., Zuo, Z., Yang, C., Castro-Palomino, J. C., Crespo, M. I., Prat, M., Gual, S., Diaz, J. L., and Saunders, J. (2008) 2-Amino-*N*-pyrimidin-4-ylacetamides as A_{2A} receptor antagonists: 1. Structure-activity relationships and optimization of heterocyclic substituents. *J. Med. Chem. 51*, 1719−1729.
(21) Slee, D. H., Moorjani, M., Zhang, X., Lin, E., Lanier, M. C., Chen, Y., Rueter, J. K., Lechner, S. M., Markison, S., Malany, S., Joswig, T., Santos, M., Gross, R. S., Williams, J. P., Castro-Palomino, J. C., Crespo, M. I., Prat, M., Gual, S., Diaz, J. L., Jalali, K., Sai, Y., Zuo, Z., Yang, C., Wen, J., O'Brien, Z., Petroski, R., and Saunders, J. (2008) 2-Amino-*N*-pyrimidin-4-ylacetamides as A_{2A} receptor antagonists: 2. Reduction of hERG activity, observed species selectivity, and structure-activity relationships. *J. Med. Chem. 51*, 1730−1739.
(22) Zhang, X., Rueter, J. K., Chen, Y., Moorjani, M., Lanier, M. C., Lin, E., Gross, R. S., Tellew, J. E., Williams, J. P., Lechner, S. M., Markison, S., Joswig, T., Malany, S., Santos, M., Castro-Palomino, J. C., Crespo, M. I., Prat, M., Gual, S., Diaz, J. L., Saunders, J., and Slee, D. H. (2008) Synthesis of N-pyrimidinyl-2-phenoxyacetamides as adenosine A_{2A} receptor antagonists. *Bioorg. Med. Chem. Lett. 18*, 1778−1783.
(23) Zhang, X., Tellew, J. E., Luo, Z., Moorjani, M., Lin, E., Lanier, M. C., Chen, Y., Williams, J. P., Saunders, J., Lechner, S. M., Markison, S., Joswig, T., Petroski, R., Piercey, J., Kargo, W., Malany, S., Santos, M., Gross, R. S., Wen, J., Jalali, K., O'Brien, Z., Stotz, C. E., Crespo, M. I., Diaz, J. L., and Slee, D. H. (2008) Lead optimization of 4-acetylamino-2-(3,5-dimethylpyrazol-1-yl)-6-pyridylpyrimidines as A_{2A} adenosine receptor antagonists for the treatment of Parkinson's disease. *J. Med. Chem. 51*, 7099−7110.
(24) Lanier, M. C., Moorjani, M., Luo, Z., Chen, Y., Lin, E., Tellew, J. E., Zhang, X., Williams, J. P., Gross, R. S., Lechner, S. M., Markison, S., Joswig, T., Kargo, W., Piercey, J., Santos, M., Malany, S., Zhao, M., Petroski, R., Crespo, M. I., Diaz, J. L., Saunders, J., Wen, J., O'Brien, Z., Jalali, K., Madan, A., and Slee, D. H. (2009) *N*-[6-Amino-2-(heteroaryl)pyrimidin-4-yl]acetamides as A_{2A} receptor antagonists with improved drug like properties and in vivo efficacy. *J. Med. Chem. 52*, 709−717.
(25) Yang, Z., Li, X., Ma, H., Zheng, J., Zhen, X., and Zhang, X. (2014) Replacement of amide with bioisosteres led to a new series of potent adenosine A_{2A} receptor antagonists. *Bioorg. Med. Chem. Lett. 24*, 152−155.
(26) Jaakola, V. P., Griffith, M. T., Hanson, M. A., Cherezov, V., Chien, E. Y., Lane, J. R., Ijzerman, A. P., and Stevens, R. C. (2008) The 2.6 angstrom crystal structure of a human A_{2A} adenosine receptor bound to an antagonist. *Science 322*, 1211−1217.
(27) Xu, F., Wu, H., Katritch, V., Han, G. W., Jacobson, K., Gao, Z.-G., Cherezov, V., and Stevens, R. C. (2011) Structure of an agonist-bound human A_{2A} adenosine receptor. *Science 332*, 322−327.
(28) Lebon, G., Warne, T., Edwards, P. C., Bennett, K., Langmead, C. J., Leslie, A. G., and Tate, C. G. (2011) Agonist-bound adenosine A_{2A} receptor structures reveal common features of GPCR activation. *Nature 474*, 521−525.
(29) Dore, A. S., Robertson, N., Errey, J. C., Ng, I., Hollenstein, K., Tehan, B., Hurrell, E., Bennett, K., Congreve, M., Magnani, F., Tate, C. G., Weir, M., and Marshall, F. H. (2011) Structure of the adenosine A_{2A} receptor in complex with ZM241385 and the xanthines XAC and caffeine. *Structure 19*, 1283−1293.
(30) Houston, J. B., and Carlile, D. J. (1997) Prediction of hepatic clearance from microsomes, hepatocytes, and liver slices. *Drug Metab. Rev. 29*, 891−922.